Quantum state of two trapped Bose-Einstein condensates with a Josephson coupling

M. J. Steel and M. J. Collett
Department of Physics, University of Auckland, Private Bag 92 019, Auckland, New Zealand
(Received 15 October 1997)

We consider the precise quantum state of two trapped, coupled Bose-Einstein condensates in the two-mode approximation. We seek a representation of the state in terms of a Wigner-like distribution on the two-mode Bloch sphere. The problem is solved using a self-consistent rotation of the unknown state to the south pole of the sphere. The two-mode Hamiltonian is projected onto the harmonic-oscillator phase plane, where it can be solved by standard techniques. Our results show how the number of atoms in each trap and the squeezing in the number difference depend on the physical parameters. Considering negative scattering lengths, we show that there is a regime of squeezing in the relative phase of the condensates which occurs for weaker interactions than the superposition states found by Cirac *et al.* (quant-ph/9706034). The phase squeezing is also apparent in mildly asymmetric trap configurations. [S1050-2947(98)06303-3]

PACS number(s): 03.75.−b

I. INTRODUCTION

Traditionally, a Bose-Einstein condensate (BEC) is often viewed as a coherent state of the atomic field with a definite phase [1]. It is well known that there are problems with this view, however, related to the fact that the phase of the atomic field is not an observable [1–4]. The Hamiltonian for the atomic field is independent of the condensate phase and so the correct coherent state is only defined up to its mean number. Often it is convenient to invoke a symmetry-breaking Bogoliubov field to select a particular phase, but this does not correspond to any physical field, so the procedure is not totally satisfactory in a formal sense. In addition, a coherent state implies a superposition of number states, whereas in the current single-trap experiments [5–8] there is a fixed number of atoms in the trap (even if we are ignorant of that number), and the state of a single trapped condensate must be a number state (or more precisely, a mixture of number states). Both these problems are bypassed by considering a system of two condensates for which the total number of atoms N is fixed. Then, a general state of the system is a superposition of number difference states of the form

$$|\ \rangle=\sum_{k=0}^{N} c_k|k,N-k\rangle. \tag{1}$$

As we now have a well-defined superposition state, we can legitimately consider the relative phase of the two condensates, which is an Hermitian observable. Indeed, the dramatic observation of interference between two coherent BEC's [9] constitutes a measurement of exactly this. In the absence of atomic collisions, the expansion coefficients in Eq. (1) obey a binomial rather than Poissonian distribution, as would be expected for a coherent state.

However, there is a more straightforward objection to the identification of the condensate with a coherent state. This is that, in real experiments, the atoms experience collisions introducing a nonlinearity into the Hamiltonian for the system. We then know immediately that (unless very strongly damped) the true state can not be a coherent state, leaving aside issues of absolute versus relative phase. In the first treatment of this question, Lewenstein and You [10] suggested that the condensate is actually in an amplitude quadrature eigenstate. In a fuller analysis, Dunningham and co-workers [11,12] showed that for positive (repulsive) interactions the state is strongly number squeezed, and resembles a bent version of the amplitude squeezed state that minimizes number fluctuations. This has the potentially observable consequence of increasing the revival time in collapses and revivals of the relative phase [13–16] due to the reduced number variance of the squeezed state. The approach of Dunningham and co-workers was based on the symmetry-breaking picture described above. Their model thus described the quantum state of a single damped driven condensate with the phase determined by some much larger reference condensate which does not appear in the calculation. Thus while the number squeezing they predicted is intuitively natural, the model faces the same formal difficulties mentioned above in relation to symmetry breaking.

In this paper, we combine these two ideas by seeking an accurate description of the ground state beyond the coherent state picture, for a system of two coupled condensates with a fixed total number of atoms. We do this by reducing the full quantum field-theoretical description to an approximate two-mode problem, valid for condensates of a few thousand atoms. The problem is then well defined in the senses discussed above: we deal with relative rather than absolute phases, and are able to consider a completely closed system without the complications of driving and damping, so that the ground state is unambiguously a pure state. Using a variational approach, we then find approximate solutions to the two-mode problem which are natural analogs of the single condensate states found by Dunningham and co-workers. Our approach also works for negative (attractive) interactions, and we predict a regime of significant phase squeezing in between the coherent-state-like behavior with no interactions, and the Schrödinger cat states reported previously [17,18] that occur with significant interactions.

The paper is structured as follows. In Sec. II we briefly summarize the quantum field theory for the two-condensate problem, and derive the approximate two-mode Hamiltonian. In Sec. III we discuss a representation of the two-mode states

using the Bloch sphere, and outline our method for finding the ground state of the system. We construct the solution in detail in Sec. IV. In Sec. V, we present our results and compare the predictions of our method with exact solutions for systems with small numbers of atoms. We consider negative scattering lengths and the associated phase squeezing in Sec. VI before we conclude.

II. GOVERNING HAMILTONIAN

A. Reduction to two-mode Hamiltonian

Our model describes two condensates of atoms of mass m, with a linear Josephson coupling and weak nonlinear interactions. We consider a single trap with the condensates distinguished by their internal atomic state [17]. The coupling is provided by laser-induced Raman transitions between the two atomic states. Following Cirac *et al.* [17], the second quantized Hamiltonian takes the form

$$H=H_1+H_2+H_{\rm int}+H_{\rm coup}, \tag{2}$$

with

$$H_j=\int d^3\mathbf{x}\ \hat{\psi}_j^\dagger(\mathbf{x})\Big[-\frac{\hbar^2}{2m}\nabla^2+V_j(\mathbf{x}) +\frac{4\pi\hbar^2 a_j}{2m}\hat{\psi}_j^\dagger(\mathbf{x})\hat{\psi}_j(\mathbf{x})\Big]\hat{\psi}_j(\mathbf{x}), \tag{3}$$

$$H_{\rm int}=\frac{4\pi\hbar^2 a_{12}}{2m}\int d^3\mathbf{x}\ \hat{\psi}_1^\dagger(\mathbf{x})\hat{\psi}_2^\dagger(\mathbf{x})\hat{\psi}_1(\mathbf{x})\hat{\psi}_2(\mathbf{x}), \tag{4}$$

$$H_{\rm coup}=-\frac{\hbar\Omega}{2}\int d^3\mathbf{x}\ [\hat{\psi}_1(\mathbf{x})\hat{\psi}_2^\dagger(\mathbf{x})e^{-i\delta t}+\hat{\psi}_1^\dagger(\mathbf{x})\hat{\psi}_2(\mathbf{x})e^{i\delta t}], \tag{5}$$

where $j=1$ and 2. Here the field operators $\hat{\psi}_1(\mathbf{x})$ and $\hat{\psi}_2(\mathbf{x})$ annihilate atoms at position $\mathbf{x}$ in condensates 1 and 2, respectively, and satisfy the relation $[\hat{\psi}_i(\mathbf{x}),\hat{\psi}_j^\dagger(\mathbf{x}')]=\delta_{ij}\delta(\mathbf{x}-\mathbf{x}')$. The term $H_{1,2}$ describes each of the condensates in the absence of interactions with the other. They experience spherical harmonic trap potentials $V_{1,2}$ of frequencies ω_1 and ω_2, and have scattering lengths a_1 and a_2, respectively. The cross-phase modulation term $H_{\rm int}$ describes collisional interactions between the condensates with scattering length a_{12}. The laser-induced coupling is described by $H_{\rm coup}$, with Ω the Rabi frequency and δ the detuning of the classical laser field. In our work, we assume equal scattering lengths $a_1=a_2=a_{12}$, but allow the trap frequencies to differ.

The procedure to obtain the two-mode Hamiltonian is well known [17,19]. We approximate the field operators as $\hat{\psi}_1(\mathbf{x})=b_1\phi_1(\mathbf{x})$ and $\hat{\psi}_2(\mathbf{x})=b_2\phi_2(\mathbf{x})$ where $\phi_{1,2}(\mathbf{x})$ are (real) normalized mode functions for the two condensates, and $b_{1,2}$ are the associated mode annihilation operators which obey the standard commutation relations $[b_i,b_j]=0$, $[b_i,b_j^\dagger]=\delta_{ij}$. Then Eq. (2) becomes

$$H\approx(\overline{\omega_1}+\delta)b_1^\dagger b_1+\overline{\omega_2}b_2^\dagger b_2+\chi_1 b_1^\dagger b_1^\dagger b_1 b_1+\chi_2 b_2^\dagger b_2^\dagger b_2 b_2 +\chi_{12}b_1^\dagger b_1 b_2^\dagger b_2-\frac{\eta}{2}(b_1 b_2^\dagger+b_1^\dagger b_2), \tag{6}$$

where

$$\overline{\omega_i}=\int d^3\mathbf{r}\ \overline{\phi_i}(\mathbf{r})\Big[-\frac{1}{2}\nabla^2+\frac{\lambda_i^2 r^2}{2}\Big]\overline{\phi_i}(\mathbf{r}), \tag{7}$$

$$\chi_i=\frac{U_i}{2}\int d^3\mathbf{r}\ |\overline{\phi_i}(\mathbf{r})|^4, \tag{8}$$

$$\chi_{12}=\frac{U_{12}}{2}\int d^3\mathbf{r}|\overline{\phi_1}(\mathbf{r})|^2|\overline{\phi_2}(\mathbf{r})|^2, \tag{9}$$

$$\eta=\frac{\Omega}{\omega_0}\int d^3\mathbf{r}\ \overline{\phi_1}(\mathbf{r})\overline{\phi_2}(\mathbf{r}) \tag{10}$$

for $i=1$ and 2. Here we have moved into the interaction picture and introduced dimensionless variables, scaling the Hamiltonian by an appropriate energy $\hbar\omega_0$ and the position by the length scale $x_0=\sqrt{\hbar/m\omega_0}$ such that $\mathbf{r}=\mathbf{x}/x_0$ and $\overline{\phi_i}(\mathbf{r})=x_0^{3/2}\phi(\mathbf{x})$. Further, $\lambda_i=\omega_i/\omega_0$, $U_i=4\pi a_i/x_0$, and $U_{12}=4\pi a_{12}/x_0$.

As shown by Milburn *et al.* [19], the same two-mode model also describes coupling between condensates in a double-well potential. In this case, the two lowest modes are, strictly speaking, the symmetric and antisymmetric modes of the entire double well, but for a strong dividing potential barrier it is an accurate approximation to use modes describing atoms in one or the other trap. The linear coupling is provided directly by spatial tunneling through the barrier and has a strength $\eta=\Delta E/\omega_0$ where ΔE is the frequency separation of the two (linear) modes [19]. Assuming the potential barrier is relatively strong, the modes are well separated, and we can neglect $H_{\rm int}$.

Equation (6) defines our problem completely. For large condensates, the mode functions are altered by the collisional interactions, and the two-mode approximation breaks down. As shown in Ref. [19], a simple estimate shows this occurs when the number of atoms N satisfies $Na\gg x_0$, where a is a typical scattering length and x_0 is a measure of the trap size. Assuming $a\approx 5$ nm [6,20] and a large trap with $x_0\approx 10\ \mu$m, we find that the two-mode approximation should be acceptable for $N<2000$.

B. Angular momentum representation

The Hamiltonian can be reduced to a simpler form by exploiting the equivalence between the algebra for two harmonic oscillators and that for angular momentum, by introducing the new operators [21,19]

$$J_+=b_1^\dagger b_2,$$

$$J_-=b_1 b_2^\dagger,$$

$$J_z=\frac{1}{2}(b_1^\dagger b_1-b_2^\dagger b_2) \tag{11}$$

and

$$J_x=\tfrac{1}{2}(J_++J_-), \tag{12}$$

$$J_y=\frac{1}{2i}(J_+-J_-), \tag{13}$$

These operators do indeed satisfy the usual angular momentum commutation relations, justifying the choice of notation. In addition, we find

$$\mathbf{J}^2=J_x^2+J_y^2+J_z^2=\frac{N}{2}\left(\frac{N}{2}+1\right), \tag{14}$$

where the total number of atoms $N=n_1+n_2=b_1^\dagger b_1+b_2^\dagger b_2$ is a constant of the motion, so we deduce that we are working with the angular momentum algebra for $J=N/2$. In terms of the new variables, Eq. (6) takes the form

$$\begin{aligned}H&=J(\overline{\omega_1}+\delta+\overline{\omega_2}-\chi_1-\chi_2)+J^2(\chi_1+\chi_2+\chi_{12})+\Delta\overline{\omega}J_z\\&\quad+\chi_+J_z^2-\frac{\eta}{2}(J_++J_-)\\&=\Delta\overline{\omega}J_z+\chi_+J_z^2-\eta J_x,\end{aligned} \tag{15}$$

where in the last line we have dropped an unimportant constant, and introduced the effective detuning

$$\Delta\overline{\omega}=\overline{\omega_1}+\delta-\overline{\omega_2}+(2J-1)\chi_- \tag{16}$$

and effective nonlinearity

$$\chi_+=\chi_1+\chi_2-\chi_{12}. \tag{17}$$

Note the useful fact that both the difference in the self-nonlinearities $\chi_-=\chi_1-\chi_2$ and the cross-nonlinearity χ_{12} merely shift the values of $\Delta\overline{\omega}$ and χ_+ and introduce no new terms. Thus there is no restriction of the physics by assuming equal scattering lengths. We now calculate these parameters for realistic experimental values. Taking the ^{23}Na atom, for example, we have $a\approx 5$ nm, and suppose trap frequencies of order $\omega_i=1000\ \mathrm{s}^{-1}$ [6]. Then taking the scaling frequency $\omega_0=1\ \mathrm{s}^{-1}$, we obtain $\overline{\omega_i}\approx 1500$ and $\chi_i\approx 1.4$. Therefore, the detuning $\Delta\overline{\omega}$ may range from zero to a few hundred. The coupling strength η is largely arbitrary. In the spatial case, it can take values up to the order of the trap frequencies [19], or can be made as small as desired by incresing the trap separation.

III. OUTLINE OF APPROACH

For the remainder of the paper we are concerned with the ground state of Eq. (15). Milburn *et al.* [19] presented numerical calculations of the energy spectrum of this Hamiltonian, and the dynamical problem was also studied [19,22]. Rather than the spectrum or dynamics, however, our concern is with the detailed properties of the lowest eigenstate and their dependence on the effective detuning and nonlinearity. In general, the eigenstates of Eq. (15) cannot be written analytically. For systems with at most a few hundred atoms, it is feasible to find the exact eigenstates in the basis of J_z eigenstates $|J,m=-J,\ldots,J\rangle_z$ numerically. Our semianalytic approach can be used for systems of arbitrary size, and lends considerable insight to the problem.

A. Bloch sphere

Our approach relies closely on the Bloch sphere representation of the angular momentum, which we must briefly introduce. A detailed analysis was given by Arecchi *et al.* [23]. Quantum states in the angular momentum Hilbert space can be usefully represented on the Bloch sphere. Certain states—the atomic coherent states or ''Bloch'' states [23]—correspond to a single point on the sphere. Defined as the rotated states $|\theta,\varphi\rangle=R_{\theta,\varphi}|J,-J\rangle_z$, where the rotation operator

$$\begin{aligned}R_{\theta,\varphi}&=\exp[\,\theta/2(J_+e^{-i\phi}-J_-e^{i\phi})\,]\\&=\exp[-i\theta(J_x\sin\varphi-J_y\cos\varphi)],\end{aligned} \tag{18}$$

they are labeled by the spherical coordinates θ and φ corresponding to the state's point on the sphere. Note that in terms of our BEC problem, the north pole $|\theta=\pi\rangle$ and south pole $|\theta=0\rangle$ represent the states with all atoms in mode 1 or 2 respectively. States lying on the equator with $\theta=\pi/2$ represent an equal division of atoms between the modes [which for $\eta\neq 0$, does *not* imply the number state $|N/2,N/2\rangle$, but rather an entanglement of form (1) with a binomial distribution of expansion coefficients]. The Bloch states are the analogs in the angular momentum algebra of the standard coherent states of the harmonic oscillator [23]. They share a number of properties with the coherent states, for instance minimum uncertainty in the natural variables. In addition, more general nonclassical states described by the state vector $|\psi\rangle$ or density matrix ρ can be naturally pictured in terms of a quasiprobability distribution function on the sphere,

$$\widetilde{Q}_{|\psi\rangle}(\theta,\varphi)=|\langle\theta,\varphi|\psi\rangle|^2, \tag{19}$$

$$\widetilde{Q}_\rho(\theta,\varphi)=\langle\theta,\varphi|\rho|\theta,\varphi\rangle, \tag{20}$$

in analogy to the familiar Q function in the harmonic-oscillator phase plane [24]. Functions analogous to the standard Glauber-Sudarshan P and Wigner distributions can also be defined. As discussed below, these analogies can be made precise using a formal contraction from the angular momentum Hilbert space to the Hilbert space for a single harmonic oscillator [23]. While the Bloch states lack some of the useful properties of the coherent states [23,25] , nonetheless, we see below that the Wigner or $\widetilde{Q}$ functions make for useful measures of quantities such as the squeezing in the number difference or relative phase in the ground state.

B. Mathematical procedure

The angular momentum commutation relations make a direct solution to our problem in the full Hilbert space difficult. Section III A suggests the following alternative approach. We assume that the ground state we seek has a quasiprobability distribution localized to a particular part of the Bloch sphere. (Thus we immediately exclude Schrödinger cat states such as those found by Cirac *et al.* [17] and Ruostekoski *et al* [18], which we treat numerically in Sec. VI.) We apply a rotation to the Hamiltonian to bring the mean value of the state to the south pole of the Bloch sphere. This must be done self-consistently, as we do not actually know the mean value of the state until we have solved the problem.

We then project the problem to the harmonic-oscillator phase plane using the contraction operation of Ref. [23]. The problem can then be solved in the plane and the ground state plotted as a Wigner distribution. Finally, we project this distribution back on to the sphere, and rotate it to the original mean value, which has by now been determined. Equivalently, we can think of the problem being solved in the oscillator phase plane that is tangent to the sphere at the mean value of the state. In Sec. IV we make these ideas precise and provide the solution.

C. Linear problem

In the absence of the nonlinear term ($\chi_+ = 0$), the problem is trivial. Hamiltonian (15) becomes

$$H = \Delta\overline{\omega} J_z - \eta J_x, \tag{21}$$

and, using the rotation relations in Appendix A, it is easy to see that the rotated Hamiltonian $H' = R_{\theta,\pi} H R_{\theta,\pi}^{-1}$, where $\tan\theta = \eta/\Delta\overline{\omega}$, is just a multiple of J_z with ground state $|J,-J\rangle_z$. Inverting the rotation, the exact ground state for the original Hamiltonian is simply the Bloch state $|\theta,\phi\rangle = |\tan^{-1}(\eta/\Delta\overline{\omega}),0\rangle$. Thus the the ground state of coupled ideal gas condensates is the entangled state analog of the coherent state. This result is well known, though it is more commonly expressed in the number difference basis [26]. As expected, for vanishing $\Delta\overline{\omega}$, the traps are equivalent, and there is an equal number of atoms in each, whereas for $\Delta\overline{\omega} \neq 0$, the ground state has more atoms in the weaker trap. Note that the relative phase of the condensates $\varphi = 0$. This is the reason for our choice of the negative sign in front of η in the original Hamiltonian (15). Even when we consider the more complicated states of the nonlinear system, we see by symmetry that the mean value of the state must still have $\varphi = 0$, simplifying the rotation operators we need to consider. In practice, the phase of η is determined by the phase of the driving laser field. By a suitable choice of coordinates we may always take it to be zero.

IV. NONLINEAR PROBLEM

A. Contraction from angular momentum to harmonic-oscillator Hilbert space

The nonlinear problem is much more involved. As indicated earlier, the first step is to perform a rotation of the Hamiltonian by an undertermined angle θ, and then project the new Hamiltonian into the harmonic oscillator phase plane with operators a and $a^\dagger$ satisfying $[a,a^\dagger] = 1$. This procedure can be made rigorous through the concept of a group contraction from the angular momentum Hilbert space to the harmonic-oscillator Hilbert space. The details can be found in Ref. [23], to which we refer the interested reader. Quoting the results, the contraction is made by the identification of operators according to

$$J_+ \to \frac{1}{c} a^\dagger, \tag{22}$$

$$J_- \to \frac{1}{c} a, \tag{23}$$

$$J_z \to a^\dagger a - \frac{1}{2c^2}, \tag{24}$$

where $c = 1/\sqrt{2J}$, and the spaces are formally identical in the limit $c \to 0$. In the same limit, we can contract eigenstates of J_z to the harmonic-oscillator number states,

$$|J,M\rangle \to |n = J + M\rangle, \tag{25}$$

and we relate the coordinates according to

$$\frac{\theta}{2}\exp(i\varphi) \to c\,\alpha. \tag{26}$$

Later we also use the quadrature operators $X = a + a^\dagger$ and $Y = -i(a - a^\dagger)$, which are the contractions of J_x and J_y, respectively. Geometrically, we visualize this contraction as a projection from the Bloch sphere to the phase plane with the south pole of the sphere coincident with the origin of the phase plane. Note that the coherent amplitude α can take values throughout the whole phase plane only in the limit $c \to 0$, and there is naturally a distortion involved in the projection. Physically, by performing the contraction we discard the knowledge that the true ladder of states is bounded at both ends rather than just the lower end. However, providing the state is localized near the south pole and $c \ll 1$ (large atom number), the distortion is small. The contraction process also maps functions from the sphere to the plane, so for instance we can identify the (rotated) Bloch sphere distribution function $\widetilde{Q}(\theta,\varphi)$ with the standard phase plane function $Q(\alpha) = \langle\alpha|\rho|\alpha\rangle$. Here we define the Wigner-like distribution on the sphere by a projection of the harmonic-oscillator Wigner distribution using Eq. (26) in reverse.

B. Variational solution

1. Gaussian part

We are at last ready to find our approximate solution to the full problem. The procedure is somewhat involved mathematically, and we state only the main intermediate steps here, leaving the details to Appendix A. The first step is to rotate Hamiltonian (15) around the positive y axis by an undetermined angle θ, and perform the contraction operation to the single oscillator phase space to find the new Hamiltonian F. Following Ref. [12], we write this Hamiltonian as

$$F = F_G + F_{\rm NG}, \tag{27}$$

in terms of a Gaussian part F_G and non-Gaussian part $F_{\rm NG}$, the latter of which satisfies the constraints

$$\langle F_{\rm NG}\rangle = 0,$$

$$\langle [a,F_{\rm NG}]\rangle = \langle [a^\dagger,F_{\rm NG}]\rangle = 0,$$

$$\langle [a,[a,F_{\rm NG}]]\rangle = \langle [a,[a^\dagger,F_{\rm NG}]]\rangle = 0. \tag{28}$$

This separation allows us to find the ground state of the Gaussian part first, and by assuming a weak nonlinearity, treat the non-Gaussian part as a perturbation. Appendix A contains the expression for the non-Gaussian part. The Gaussian part is

$$F_G = K + L(a + a^\dagger) + Sa^\dagger a + T(a^2 + a^{\dagger 2}), \tag{29}$$

where

$$K = \chi_+ J/2 \sin^2\theta + \chi_+ J^2 \cos^2\theta - J(\Delta\overline{\omega} \cos\theta + \eta \sin\theta) + 2\sqrt{2J}\chi_+ \cos\theta \sin\theta \langle a^\dagger a^2\rangle + \chi_+ \cos^2\theta(\langle a^{\dagger 2} a^2\rangle - 2\langle a^2\rangle^2 - 4\langle a^\dagger a\rangle^2), \tag{30}$$

$$L = \sqrt{\frac{J}{2}}\{\Delta\overline{\omega} \sin\theta - \eta \cos\theta + \chi_+ \sin\theta \cos\theta[-(2J-1) + 2\langle a^2\rangle + 4\langle a^\dagger a\rangle]\}, \tag{31}$$

$$S = \eta \sin\theta + \Delta\overline{\omega} \cos\theta + \chi_+\{J \sin^2\theta + \cos^2\theta[-(2J-1) + 4\langle a^\dagger a\rangle]\}, \tag{32}$$

$$T = \chi_+\left(\frac{J}{2}\sin^2\theta + \cos^2\theta\langle a^2\rangle\right). \tag{33}$$

In Eqs. (30)–(33), we took $\langle a^2\rangle = \langle a^{\dagger 2}\rangle$, which follows from the choice of η as real. Note that F_G depends on moments taken over the state which is the solution we are seeking. We can solve the Gaussian part to different levels of accuracy according to how we account for these expectation values.

(a) Non-self-consistent approach. We first assume we have known values for the expectation values. For example, we may take a mean-field approximation in which all the moments are zero, or as explained below we may have obtained estimates for the moments from a previous less accurate calculation (such as the mean-field one). We consider a self-consistent approach in Sec. IV B 2. The rotation angle θ is fixed by requiring that the linear terms should vanish,

$$L = 0. \tag{34}$$

Except for a constant term, F_G is now purely quadratic, and we perform a Boguliobov diagonalization by writing

$$a = b \cosh r - b^\dagger \sinh r,$$

$$a^\dagger = b^\dagger \cosh r - b \sinh r. \tag{35}$$

Substituting Eqs. (35) into Eq. (29) and setting the terms in b^2 and $b^{\dagger 2}$ to zero, we obtain

$$\exp(-2r) = \sqrt{\frac{S-2T}{S+2T}}, \tag{36}$$

while the diagonalized Hamiltonian is

$$F_G = K + (S \cosh^2 r - 2T \cosh r \sinh r) + \sqrt{S^2 - 4T^2}\, b^\dagger b. \tag{37}$$

The first two terms are constants, so the ground state is just the vacuum in the b representation. As the transformation (35) is induced by the squeezing operator $S(r) = \exp[r(a^2 - a^{\dagger 2})/2]$ [24], the b eigenstates $|i\rangle$ transform back as

$$|\tilde{i}\rangle_a = S(r)|i\rangle. \tag{38}$$

Thus the ground state in the a representation is just the squeezed vacuum with

$$\langle X^2\rangle = \exp(-2r) = \sqrt{\frac{S-2T}{S+2T}}. \tag{39}$$

In the mean-field limit we have the simple results

$$\Delta\overline{\omega} = \eta \cot\theta + \chi_+ \cos\theta(2J-1), \tag{40}$$

$$\langle X^2\rangle = \sqrt{\frac{\eta}{\eta + N\chi_+ \sin^3\theta}}. \tag{41}$$

For $\Delta\overline{\omega} = 0$, we find symmetric states with $\theta = \pi/2$ as is natural. Moreover, in the limit $\theta \to \pi/2$ (that is, for $\Delta\overline{\omega}/[(2J-1)\chi_+] \to 0$), the non-Gaussian part of the Hamiltonian $F_{\rm NG} = 0$ (see Appendix A) and F_G is independent of any expectation values. Thus in this limit, the projected state is *exactly* a squeezed state with $\langle X^2\rangle = \sqrt{\eta/(\eta + \chi_+ N)}$. We note in passing that for a negative nonlinearity, Eq. (41) predicts $\langle X^2\rangle > 1$, which indicates a possibility of phase-squeezing. We return to this in Sec. VI.

(b) Self-consistent approach. We can also find the ground state of Eq. (29) with a self-consistent approach in which the expectation values are determined to Gaussian approximation in the course of the calculation. In this case, the first two terms in Eq. (37) can not be considered constants, and in general the b vacuum is not the lowest eigenstate. The correct approach is to assume a squeezed vacuum solution $|r\rangle = S(r)|0\rangle$ to Eq. (29), and find θ and r by minimizing the expectation value of the energy subject to the constraint in Eq. (34). Performing transformation (35) with this value of r gives a Hamiltonian in the b representation with a small off-diagonal part which can be transfered to the non-Gaussian part $F_{\rm NG}$ yet to be treated. In fact, we have found that we can obtain virtually identical results by proceeding directly with the Boguliobov diagonalization, and solving Eqs. (34) and (39) simultaneously for θ and r, where L, S, and T now depend on r through the quadratic moments.

2. Non-Gaussian part

We now include the effects of the non-Gaussian part $F_{\rm NG}$ as a perturbation to the squeezed state just found. We use second-order perturbation theory to write the corrected state as

$$|\Phi^{(2)}\rangle_a = |\tilde{0}\rangle_a + \sum_{k\neq 0} \frac{{}_a\langle \tilde{k}|F_{\rm NG}|\tilde{0}\rangle_a}{E_0^{(0)}-E_k^{(0)}}|\tilde{k}\rangle_a \tag{42}$$

$$+\sum_{k\neq 0}\left\{\left[\sum_{l\neq 0}\frac{{}_a\langle \tilde{k}|F_{\rm NG}|\tilde{l}\rangle_{aa}\langle \tilde{l}|F_{\rm NG}|\tilde{0}\rangle_a}{(E_0^{(0)}-E_k^{(0)})(E_0^{(0)}-E_l^{(0)})}\right]-\frac{{}_a\langle \tilde{k}|F_{\rm NG}|\tilde{0}\rangle_{aa}\langle \tilde{0}|F_{\rm NG}|\tilde{0}\rangle_a}{(E_0^{(0)}-E_k^{(0)})^2}\right\}|\tilde{k}\rangle_a, \tag{43}$$

where from Eq. (37) $E_k^{(0)}=k\sqrt{S^2-4T^2}$ is the energy of the unperturbed state $|\tilde{k}\rangle_a$. We then calculate the Wigner distribution

$$W(\alpha)=\frac{1}{\pi^2}\int d^2z\; e^{\alpha z^*-\alpha^* z}\chi(z), \tag{44}$$

where the symmetric characteristic function is $\chi(z)=\mathrm{Tr}\{\rho_a \exp(za^\dagger - z^* a)\}$ and $\rho_a=|\Phi^{(2)}\rangle_{aa}\langle\Phi^{(2)}|$. The details of these calculations are given in Appendix B. The final answer has a closed form in terms of Hermite Gaussians but is too long to write here.

3. Combined approach

In finding ground states, we used the above steps in an iterative scheme. A first approximation is found using the self-consistent approach to the Gaussian part followed by the perturbation theory. The quadratic moments appearing in Eqs. (34) and (39) [through L, S, and T] are calculated using this first approximation, and a new Gaussian state is chosen. Finally the perturbation theory is applied again.

4. Antirotation

To complete the problem, the contours of the Wigner function just obtained must be projected back to the sphere and the original rotation of the Hamiltonian by angle θ reversed. This is completely elementary and we reserve the equations for Appendix C.

V. RESULTS

A. Exact states

In this section, we present a mixture of exact numerical results and those obtained by our semianalytic procedure. This allows us to test the agreement in the regime where the size of the Hilbert space is small enough to permit a complete numerical solution. To begin, in Fig. 1, we show three sample exact states for $N=100$ atoms plotted as contours of Wigner functions on the surface of the Bloch sphere. There are two contours for each state at heights e^{-1} and $e^{-1}/4$ of the maximum of the Wigner function. States (a) and (b) show states with a nonlinearity $\chi_+=0.75$ and detuning $\Delta\omega=0$ and 30, respectively. Both states show strong squeezing in the number difference (the vertical axis J_z), while for the asymmetric case (b) the atoms are predominantly found in the trap of lower energy. Note that the sense of squeezing is along parallels of latitude and not along the great circle through the mean-field point. This is rather obvious—we expect squeezing along the number difference axis J_z, but it has the effect that the states are in most cases far from minimum uncertainty in the natural variables. We discuss this shortly. For comparison, state (c) is just the Bloch state solution to the linear problem ($\chi_+=0$), with $\Delta\omega=-0.44$, for which the contours are circles. Note that the mean angle θ is the same distance from the equator $\theta=\pi/2$ for states (b) and (c) despite very different values of the magnitude of the detuning $|\Delta\omega|$. As indicated by Eq. (40), the positive nonlinearity tends to push states back toward the equator and is balanced by a much larger value of the detuning. This derives from an energy competition between the terms in $\langle J_z\rangle$ and $\langle J_z^2\rangle$ in Hamiltonian (15).

B. Comparison with the model

We illustrate the results of our semianalytic method by rotating the nonlinear states (a) and (b) in Fig. 1 to the south pole, and projecting them to the plane in Figs. 2(a) and 2(b), respectively. The contours are at $e^{-1}/2$ of the maximum of the Wigner function. Here we see the effect of the fact that the orientation of the squeezing is along the parallels of latitude. The state originally at $\theta=\pi/2$ [Fig 1(a)] is a precise squeezed state with no bending, but the asymmetric state in Fig. 1(b) is distorted on projection [solid line in Fig. 2(b)]. The other lines in Fig. 2(b) indicate our semianalytic prediction to second-order perturbation theory. The dashed line shows the solution using the mean-field approximation for the expectation values in Eqs. (30)–(33). The dot-dashed line is for the improved result in which the expectation values are first estimated using the self-consistent approach. The bending we find here is a clear analog of that found for a single

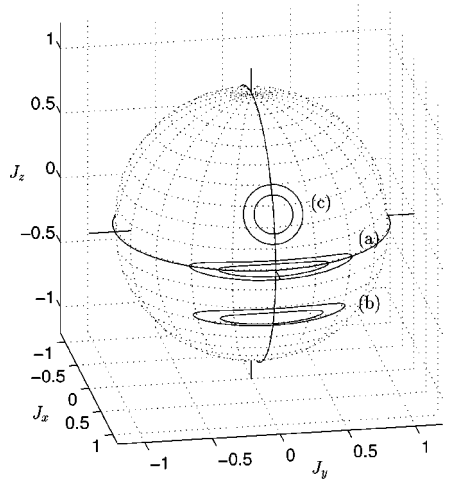

FIG. 1. Contours of the Wigner function on the Bloch sphere for exact solutions with $N=100$ atoms and (a) detuning $\Delta\bar{\omega}=0$, nonlinearity $\chi_+=0.75$; (b) $\Delta\bar{\omega}=30$, $\chi_+=0.75$; and (c) $\Delta\bar{\omega}=-0.44$, $\chi_+=0$.

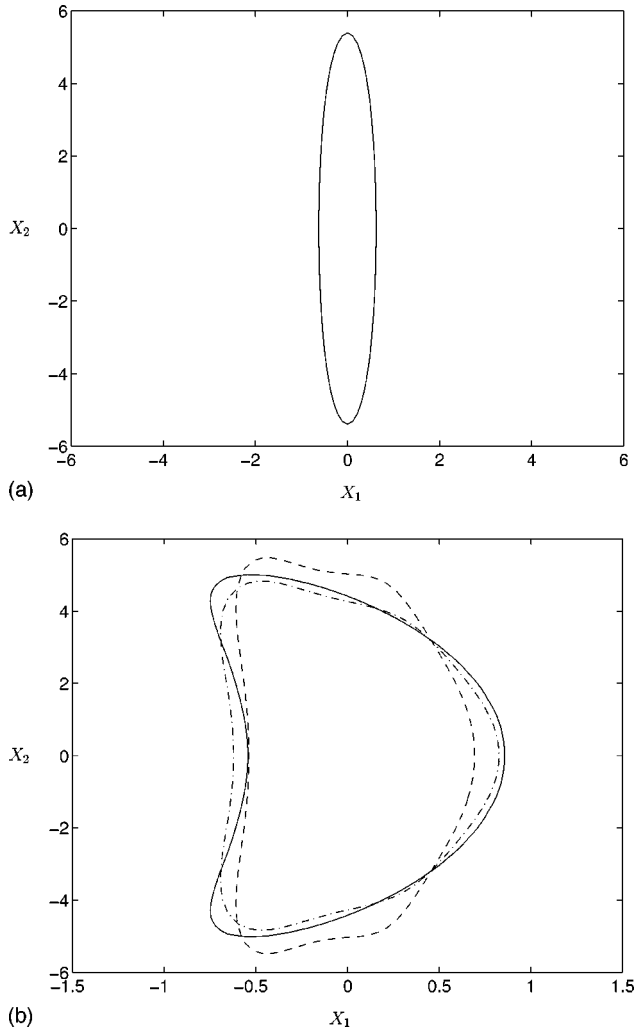

FIG. 2. Contours of the Wigner function projected into the plane for states (a) and (b) in Fig. 1. The solid lines are the exact results. In (b), we also show the prediction of the mean-field approximation (dashed line), and that using corrected versions of the quadratic moments (dot-dashed line).

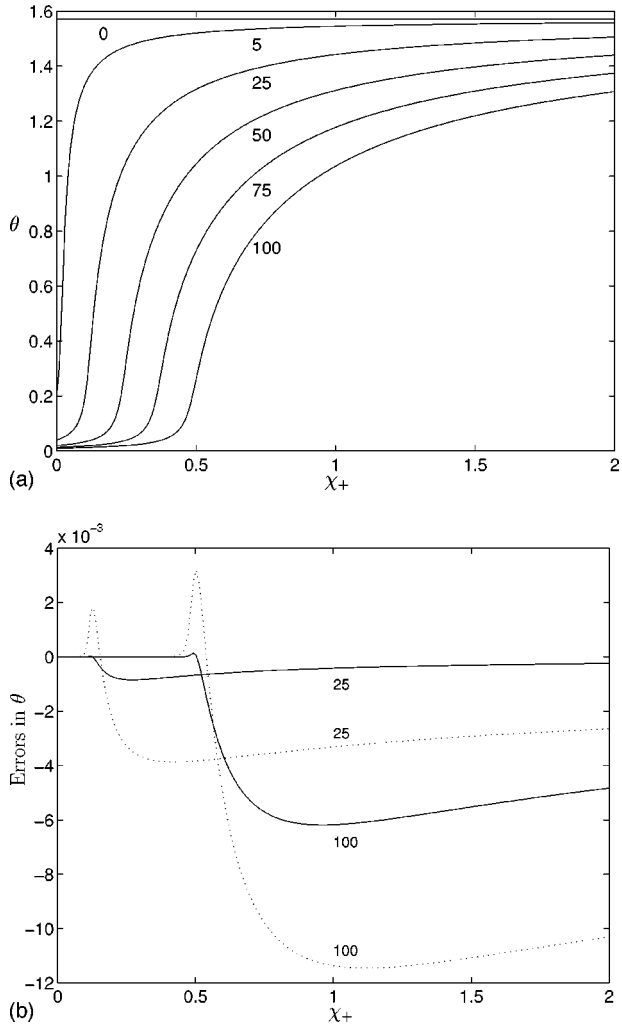

FIG. 3. (a) Mean angular position θ as a function of nonlinearity χ_+ for $\Delta\overline{\omega}=0$, 25, 50, 75, and 100. (b) Discrepancy in the mean angle θ from the exact result as calculated by the mean-field picture (dotted) and corrected moments picture (solid). The curves are labeled by the detuning $\Delta\overline{\omega}$.

condensate in Ref. [12], but in our case arises purely from the geometric effect of projection. As our theory gives the exact symmetric state, the lines are coincident in Fig. 2(a).

The dependence of the mean angular position of the state $\theta=\tan^{-1}(-\langle J_x\rangle/\langle J_z\rangle)$ on the detuning and nonlinearity for exact solutions with $N=200$ is shown in Fig. 3(a). This, of course, is a measure of the imbalance in the populations of each trap: $\langle n_1\rangle=J(1-\cos\theta)$ and $\langle n_2\rangle=J(1+\cos\theta)$. We plot the mean angle θ as a function of the nonlinearity χ_+ for detunings of $\Delta\overline{\omega}=0$, 5, 25, 50, 75, and 100 which label the curves. As χ_+ increases, the mean value increases from the linear result $\eta=\tan^{-1}(\eta/\Delta\overline{\omega})$ toward the symmetric value $\theta=\pi/2$, with the curves for larger detuning shifting at larger nonlinearities. From Eq. (40), we see that the most rapid change occurs for $\chi_+\approx\Delta\overline{\omega}(2J-1)$. As explained above, the tendency toward symmetric states is a result of an increasing energy penalty for asymmetric states from the $\langle J_z^2\rangle$ term in the Hamiltonian. We check the accuracy of our model in Fig. 3(b) showing the discrepancy in the mean angle θ according to the mean-field (dotted line) and self-consistent predictions (solid line), from the exact value calculated numerically. The curves are labeled with the value of the detuning $\Delta\overline{\omega}$. There is a clear improvement over the self-consistent case, though it is less dramatic for the larger detuning.

We consider the behavior of the spread in number difference $\delta n=\sqrt{\mathrm{Var}(n_1-n_2)}=4\sqrt{\mathrm{Var}(J_z)}$ for the same parameters in Fig. 4. The solid lines are the exact result, the dotted lines our approximate result using the corrected quadratic moments, and again the curves are labeled by the detuning $\Delta\overline{\omega}$. For $\Delta\overline{\omega}=0$, the state is always centered on the equator and the number squeezing grows stronger with the nonlinearity. For this case, in the limit $c\to 0$, when the projection gives the exact solution, we have $\delta n=\sqrt{N}[\eta/(\eta+\chi_+N)]^{1/4}$. The discrepancy of this curve from the exact result is not visible in Fig. 4. The behavior is somewhat different for the other cases. Initially the spread in number increases, before turning around and becoming coincident with the decreasing symmetric case. The initial rise in the variance agrees closely with the Bloch state result $\delta n=$

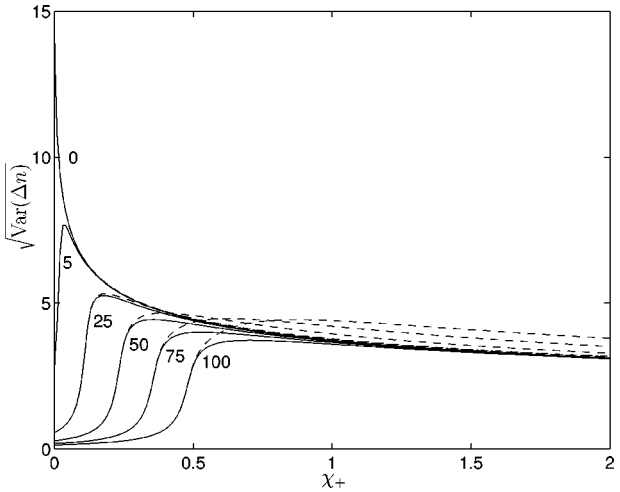

FIG. 4. Spread in the number difference $\delta n=[\mathrm{var}(n_1-n_2)]^{1/2}$. Solid lines are exact results, and dotted lines are predictions of the corrected moments theory. The curves are labeled by the detuning $\Delta\bar{\omega}$

$\sqrt{N\sin\theta}$ (not shown in figure) until just before the maxima of the curves. Thus we see that initially the nonlinearity shifts the mean value of the state without affecting its shape. In this plot, we see that our approximate method is less successful for cases with large detunings. These states are highly asymmetric, and therefore the projected states show significant bending. The perturbation from the Gaussian squeezed state is thus larger and our calculation less accurate.

VI. NEGATIVE NONLINEARITIES

We demonstrate briefly here that for a negative nonlinearity there is a regime of phase squeezing rather than number squeezing. Using a mean-field picture, Cirac *et al.* [17] found a range of superposition states for negative nonlinearities (attractive interactions). They showed the two lowest-energy states are even and odd superpositions of states in which most of the atoms are in trap 1 or most are in trap 2. In our notation they arise as follows. In the mean-field approximation of Eq. (40), and taking the symmetric case $\Delta\bar{\omega}=0$, we have

$$\sin\theta=\frac{-\eta}{\chi_+(N-1)}. \tag{45}$$

This equation clearly only has solutions for $|\chi_+|$ sufficiently large. When this is true, there are two degenerate mean-field ground states $|\theta,0\rangle$ and $|\pi-\theta,0\rangle$. Cirac *et al.* showed that the superposition or ''Schrödinger'' cat states $|\pm\rangle=(1/\sqrt{2})(|\theta,0\rangle\pm|\pi-\theta,0\rangle)$ give a lower value for the energy, and

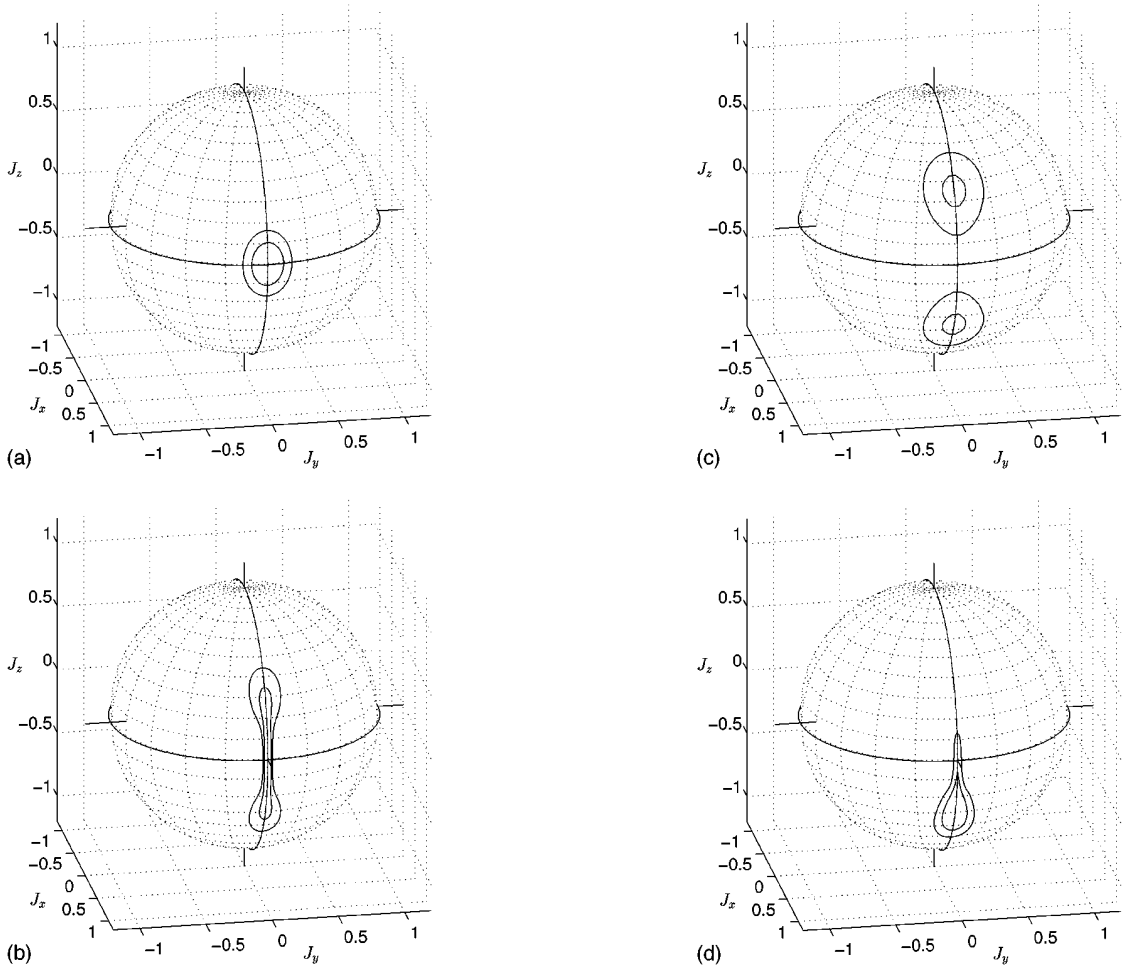

FIG. 5. Exact states for negative nonlinearities. (a) Wigner function for $\chi_+=-0.01$ and $\Delta\bar{\omega}=0$. (b) Wigner function for $\chi_+=-0.0115$ and $\Delta\bar{\omega}=0$. (c) $\tilde{Q}$ function for $\chi_+=-0.012$ and $\Delta\bar{\omega}=0$. (d) Wigner function for $\chi_+=-0.0115$ and $\Delta\bar{\omega}=0.001$.

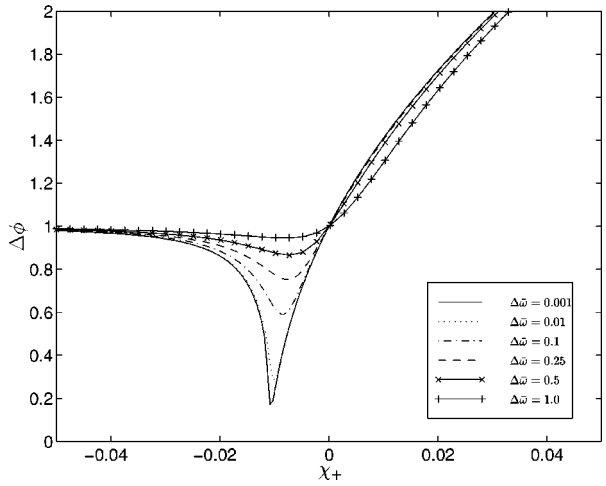

FIG. 6. Relative phase variance $\Delta\phi=(\langle J_y^2\rangle-\langle J_y\rangle^2)/(J/2)$ as a function of nonlinearity χ_+. The legend indicates line types for different detunings.

thus are a better approximation to the lowest energy levels. Ruostekoski and Walls [18] proposed a scheme for generating similar superpositions in number for free condensates. Numerically, we have found that the exact ground states in this regime are indeed of a superposition nature, though of course they are superpositions of distorted Bloch states, not of true Bloch states. What about the regime $\eta>|\chi_+|(2J-1)$ for which Eq. (45) has no solutions? Equations (40) and (41) give solutions with $\theta=\pi/2$ and $\langle X^2\rangle>1$. As in the Gaussian approximation the states have minimum uncertainty, we are led to expect phase squeezing. While our method is applicable for negative nonlinearities, the states can be highly non-Gaussian, and the variational method is not always very successful. Therefore we use numerical results to indicate that the phase squeezing does indeed occur. We reduce the number of atoms to $N=100$ to make squeezing more obvious in the figures. Thus in the mean-field approximation, we expect superposition states for $\chi_+<-1/99\approx-0.0101$. In Figs. 5(a) and 5(b) we show the Wigner function for a succession of states with $\Delta\bar{\omega}=0$, and nonlinearities (a) $\chi_+=-0.01$ and (b) $\chi_+=-0.0115$. For a vanishing nonlinearity we have circles centered on the equator. The state becomes increasingly elongated in the number difference direction and strongly squeezed in the relative phase direction around the equator. Note that state (b) lies in the range where the mean-field picture predicts a cat state. With a further increase to $\chi_+=-0.012$, the phase squeezed state bifurcates to the cat state. This is seen in Fig. 5(c), where we plot the $\tilde{Q}$ function rather than the Wigner function to avoid interference fringes. In Fig. 5(d) we treat an asymmetric case with $\Delta\bar{\omega}=0.001$ and $\chi_+=-0.0115$. Here the energy gained by adopting the superposition state is outweighed by the energy difference between the two traps, and the lowest-energy state is a single drawn out ''teardrop.'' The extended tail is clearly a vestige of the superposition states that are favorable for vanishing or very small asymmetries. The long tail and phase squeezing may be thought of as a ''best attempt'' to attain a catlike state. In Fig. 6 we show the phase variance $\Delta\phi=(\langle J_y^2\rangle-\langle J_y\rangle^2)/(J/2)$ as a function of the nonlinearity for several values of the detuning $\Delta\bar{\omega}$. For small asymmetries there is strong phase squeezing. At larger detunings, the system is too far from the superposition state regime, and the residual phase squeezing is quenched out.

VII. CONCLUSION

In this paper we studied the quantum statistics of the ground state of a two-mode model for coupled Bose-Einstein condensates. We found strong squeezing of the number difference for positive nonlinearities and a regime of squeezing in the relative phase for negative nonlinearities. Within the validity of the two-mode approximation, our model can treat systems of arbitrary numbers of atoms. However, its applicability is limited by the eventual distortion of the condensate mode functions that occurs for condensates of more than a few thousand atoms. In order to treat larger condensates, one must account for a larger number or possibly all of the trap modes. This might be attempted by a variational solution of the full second-quantized Hamiltonian. In this fashion, Cirac *et al.* [17] calculated the energies of superposition state, while Spekkens and Sipe [27] considered the coherence properties of double traps, but neither discussed the detailed shape of the ground state. Other authors are currently using stochastic simulations of generalized Gross-Pitaevski equations with additional quantum noise terms to account for the higher modes [28].

ACKNOWLEDGMENTS

We acknowledge support of the Marsden fund of the Royal Society of New Zealand, the University of Auckland Research Committee, and the New Zealand Lotteries' Grants Board.

APPENDIX A: SEPARATION OF THE CONTRACTED HAMILTONIAN

Here we provide a fuller account of some of the steps in finding the ground state in the single oscillator Hilbert space. We first note that the rotation operator (18) transforms J_x and J_z as

$$R_{\theta,\pi}J_xR_{\theta,\pi}^{-1}=J_x\cos\theta-J_z\sin\theta, \tag{A1}$$

$$R_{\theta,\pi}J_zR_{\theta,\pi}^{-1}=J_x\sin\theta+J_z\cos\theta. \tag{A2}$$

Using these relations, we rotate the original Hamiltonian (15) to obtain

$$\begin{aligned}H'=R_{\theta,\pi}HR_{\theta,\pi}^{-1}&=J_x(\Delta\bar{\omega}\sin\theta-\eta\cos\theta)\\&+J_z(\Delta\bar{\omega}\cos\theta+\eta\sin\theta)+\chi_+[J_x^2\sin^2\theta+J_z^2\cos^2\theta\\&+\sin\theta\cos\theta(J_xJ_z+J_zJ_x)].\end{aligned} \tag{A3}$$

Performing the contraction to the harmonic-oscillator Hilbert space, we find the new Hamiltonian

$$F=\chi_+ J\left(\frac{1}{2}\sin^2\theta+J\cos^2\theta\right)-J(\eta\sin\theta+\Delta\overline{\omega}\cos\theta)$$
$$+(a+a^\dagger)\sqrt{\frac{J}{2}}[\Delta\overline{\omega}\sin\theta-\eta\cos\theta-\chi_+\sin\theta\cos\theta$$
$$\times(2J-1)]+(a^2+a^{\dagger 2})\chi_+\frac{J}{2}\sin^2\theta+a^\dagger a\{\eta\sin\theta$$
$$+\Delta\overline{\omega}\cos\theta+\chi_+[J\sin^2\theta-(2J-1)\cos^2\theta]\}$$
$$+(a^\dagger a^2+a^{\dagger 2}a)\chi_+\sqrt{2J}\sin\theta\cos\theta+a^{\dagger 2}a^2\chi_+\cos^2\theta. \tag{A4}$$

Separating F into Gaussian and non-Gaussian parts by imposing the constraints in Eqs. (28) gives

$$F_G=\chi_+\left(\frac{J}{2}\sin^2\theta+\cos^2\theta(J^2-\langle a^2\rangle^2-2\langle a^\dagger a\rangle^2)\right)$$
$$-J(\eta\sin\theta+\Delta\overline{\omega}\cos\theta)+(a+a^\dagger)\sqrt{\frac{J}{2}}\{\Delta\overline{\omega}\sin\theta$$
$$-\eta\cos\theta+\chi_+\sin\theta\cos\theta[-(2J-1)+2\langle a^2\rangle$$
$$+4\langle a^\dagger a\rangle]\}+(a^2+a^{\dagger 2})\chi_+\left(\frac{J}{2}\sin^2\theta+\cos^2\theta\langle a^2\rangle\right)$$
$$+a^\dagger a(\eta\sin\theta+\Delta\overline{\omega}\cos\theta+\chi_+\{J\sin^2\theta$$
$$+\cos^2\theta[-(2J-1)+4\langle a^\dagger a\rangle]\}) \tag{A5}$$

and

$$F_{\rm NG}=(a^\dagger a^2+a^{\dagger 2}a)\chi_+\sqrt{2J}\sin\theta\cos\theta+a^{\dagger 2}a^2\chi_+\cos^2\theta$$
$$-(a+a^\dagger)\chi_+\sqrt{2J}\sin\theta\cos\theta(\langle a^2\rangle+2\langle a^\dagger a\rangle)$$
$$-(a^2+a^{\dagger 2})\chi_+\cos^2\theta\langle a^2\rangle-a^\dagger a4\chi_+\cos^2\theta\langle a^\dagger a\rangle$$
$$+\chi_+\cos^2\theta(\langle a^2\rangle^2+2\langle a^\dagger a\rangle^2). \tag{A6}$$

In these expressions, we have taken $\langle a^2\rangle=\langle a^{\dagger 2}\rangle$, which must be true by symmetry ($\langle\varphi\rangle=0$).

APPENDIX B: EFFECTS OF THE NONGAUSSIAN HAMILTONIAN

Here we show the details of the perturbation calculation to find the effects of the non-Gaussian part of the Hamiltonian $F_{\rm NG}$. We show working only for the first-order correction. The second-order calculation proceeds identically but is much longer. We begin with the expression for the first-order perturbation to the Gaussian ground state:

$$|\Phi^{(1)}\rangle_a=|\widetilde{0}\rangle_a+\sum_{k\neq 0}\frac{{}_a\langle\widetilde{k}|F_{\rm NG}|\widetilde{0}\rangle_a}{E_0^{(0)}-E_k^{(0)}}|\widetilde{k}\rangle_a. \tag{B1}$$

It is easier to work in the b representation with the state

$$|\Phi^{(1)}\rangle_b=|0\rangle+\sum_{k\neq 0}\frac{\langle k|F_{\rm NG}|0\rangle}{E_0^{(0)}-E_k^{(0)}}|0\rangle, \tag{B2}$$

where F_{NG} must be expressed in the b basis. Applying the Bogoliubov transformation (35), we obtain

$$F_{\rm NG}=\chi_+\cos^2\theta[c^2s^2(b^{\dagger 4}+b^4)-(c^3s+cs^3)(b^{\dagger 3}b+b^\dagger b^3)$$
$$+(c^4+s^4+4c^2s^2)b^{\dagger 2}b^2]+\chi_+\sqrt{2J}\sin\theta\cos\theta$$
$$\times[(cs^2-c^2s)(b^{\dagger 3}+b^3)+(c^3-s^3+2cs^2-2c^2s)$$
$$\times(b^{\dagger 2}b+b^\dagger b^2)]+\Delta(b^{\dagger 2}+b^2), \tag{B3}$$

where $c=\cosh r$ and $s=\sinh r$, and $\Delta=T(c^2+s^2)-csS$ accounts for any quadratic part left over from the self-consistent approach. We have typically found this to be negligibly small. Substituting Eq. (B3) in Eq. (B2), we find the unnormalized new state as

$$|\Phi^{(1)}\rangle=k_0|0\rangle+k_2|2\rangle+k_3|3\rangle+k_4|4\rangle, \tag{B4}$$

with

$$k_0=1, \tag{B5}$$

$$k_2=-\frac{\Delta}{\sqrt{2}\sqrt{S^2-4T^2}} \tag{B6}$$

$$k_3=-\sqrt{\frac{2}{3}}\frac{\chi_+\sqrt{2J}\sin\theta\cos\theta(cs^2-c^2s)}{\sqrt{S^2-4T^2}}, \tag{B7}$$

$$k_4=-\sqrt{\frac{3}{2}}\frac{\chi_+\cos^2\theta c^2s^2}{\sqrt{S^2-4T^2}}. \tag{B8}$$

Setting the density matrix $\rho_a=|\Phi^{(1)}\rangle_{aa}\langle\Phi^{(1)}|$, we define the characteristic function

$$\chi(z)=\mathrm{Tr}\{\rho_a e^{za^\dagger-z^*a}\}=\mathrm{Tr}\{S^\dagger(r)\rho_a S(r)S^\dagger(r)e^{za^\dagger-z^*a}S(r)\}$$
$$=\mathrm{Tr}\{\rho_b e^{b^\dagger(zc+z^*s)-b(zs+z^*c)}\}$$
$$=\sum_{\{i,j\}\in\{0,2,3,4\}}k_ik_j\langle i|e^{b^\dagger(zc+z^*s)}e^{-b(zs+z^*c)}|j\rangle$$
$$\times\exp[-(zc+z^*s)(zs+z^*c)/2], \tag{B9}$$

from which the Wigner function is found as

$$W(\alpha)=\frac{1}{\pi^2}\int e^{\alpha z^*-\alpha^* z}\chi(z)d^2z. \tag{B10}$$

Expanding the exponential in the expectation value of Eq. (B9) and using Rodrigues' formula for the Hermite polynomials $H_n(x)=(-1)^n\exp(x^2)d^n/dx^n\exp(-x^2)$ [29], one finds that the Wigner function has a closed-form expression as a sum of two-dimensional harmonic-oscillator functions. This makes for rapid numerical calculation, but the expression is too lengthy to warrant inclusion.

APPENDIX C: INVERSE ROTATION OF DISTRIBUTIONS ON THE SPHERE

Suppose a contour $\mathcal{C}_0^p$ of the Wigner function in the plane is parametrized as

$$\mathcal{C}_0^p(t)=(x_0(t),y_0(t)), \tag{C1}$$

where $x=\alpha+\alpha^*$ and $y=-i(\alpha-\alpha^*)$ are quadrature variables. Projecting onto the sphere using the inverse of Eq. (26) we obtain

$$\theta_0(t)=c\sqrt{x_0^2(t)+y_0^2(t)}, \tag{C2}$$

$$\varphi_0(t)=\tan^{-1}\left(\frac{y_0(t)}{x_0(t)}\right), \tag{C3}$$

where care must be taken in determining the correct quadrant of φ_0. In Cartesian coordinates, the contour on the sphere is expressed

$$\mathcal{C}_0^s=(j_x(t),j_y(t),j_z(t))=J(\sin\theta_0\cos\varphi_0,\sin\theta_0\sin\varphi_0,-\cos\theta_0), \tag{C4}$$

and is transformed by the rotation to

$$\mathcal{C}_1^s=(j_x\cos\theta-j_z\sin\theta,j_y,j_x\sin\theta+j_z\cos\theta), \tag{C5}$$

which may then be reexpressed in terms of new spherical coordinates θ_1 and φ_1. Finally, if θ is small so that the number of atoms in trap 2 greatly exceeds that in trap 1, we can obtain a Wigner contour for the state of a ''single'' condensate by projecting the contour $\mathcal{C}_1^s(\theta_1,\varphi_1)$ *directly* back to the plane using Eq. (26).

[1] S. M. Barnett, K. Burnett, and J. A. Vaccarro, J. Res. Natl. Inst. Stand. Technol. **101**, 593 (1996).
[2] A. J. Leggett and F. Sols, Found. Phys. **21**, 353 (1991).
[3] A. J. Leggett, in *Bose-Einstein Condensation*, edited by A. Griffin, D. W. Snoke, and S. Stringari (Cambridge University Press, Cambridge, 1995), Chap. 19, pp. 452–462.
[4] H. Wiseman, Phys. Rev. A **56**, 2068 (1997).
[5] M. H. Anderson *et al.*, Science **269**, 198 (1995).
[6] K. B. Davis *et al.*, Phys. Rev. Lett. **75**, 3969 (1995).
[7] J. R. Ensher *et al.*, Phys. Rev. Lett. **77**, 4984 (1996).
[8] C. C. Bradley, C. A. Sackett, and R. G. Hulet, Phys. Rev. Lett. **78**, 985 (1997).
[9] M. R. Andrews *et al.*, Science **275**, 637 (1997).
[10] M. Lewenstein and L. You, Phys. Rev. Lett. **77**, 3489 (1996).
[11] J. A. Dunningham, Master's thesis, University of Auckland, 1997 (unpublished).
[12] J. A. Dunningham, M. J. Collett, and D. F. Walls, Phys. Rev. A **55**, 1398 (1997).
[13] E. M. Wright, D. F. Walls, and J. C. Garrison, Phys. Rev. Lett. **77**, 2158 (1996).
[14] T. Wong, M. J. Collett, and D. F. Walls, Phys. Rev. A **54**, R3718 (1996).
[15] E. M. Wright *et al.*, Phys. Rev. A **56**, 591 (1997).
[16] M. J. Steel and D. F. Walls, Phys. Rev. A **56**, 3282 (1997).
[17] J. I. Cirac, M. Lewenstein, K. Mølmer, and P. Zoller, quant-ph/9706034.
[18] J. Ruostekoski, M. J. Collett, R. Graham, and D. F. Walls, Phys. Rev. A **57**, 511 (1988).
[19] G. J. Milburn, J. Corney, E. M. Wright, and D. F. Walls, Phys. Rev. A **55**, 4318 (1997).
[20] D. S. Jin *et al.*, Phys. Rev. Lett. **77**, 420 (1996).
[21] J. J. Sakurai, *Modern Quantum Mechanics* (Addison-Wesley, Reading, MA, 1994).
[22] N. Korolkova and J. Peřina, Opt. Commun. **136**, 135 (1997).
[23] F. T. Arecchi, E. Courtens, R. Gilmore, and H. Thomas, Phys. Rev. A **6**, 2211 (1972).
[24] D. F. Walls and G. J. Milburn, *Quantum Optics* (Springer-Verlag, Berlin, 1994).
[25] For example, the more complicated commutation relations of angular momentum mean that the Bloch states are not the eigenstates of a simple ''annihilation'' operator, and the $\widetilde{Q}$ function defined in Eqs. (19) and (20) does not generate antinormally ordered moments of the operators J_-, J_z, and J_+, as might be hoped.
[26] K. Mølmer, Phys. Rev. A **55**, 3195 (1997).
[27] R. W. Spekkens and J. E. Sipe (private communication).
[28] M. K. Olsen (personal communication).
[29] M. A. Abramowitz and I. A. Stegun, *Handbook of Mathematical Functions* (Dover, New York, 1972).